



## Numerical Investigations about Flow Resistance Values for Stirling Type Pulse Tube Cryocooler

Onkar Joshi<sup>1,\*</sup>, Mandar Tendolkar<sup>2</sup>

<sup>1</sup> Mechanical Engineering Department, Veermata Jijabai Technological Institute, Mumbai, Maharashtra, India

<sup>2</sup> Mechanical Engineering Department, Veermata Jijabai Technological Institute, Mumbai, Maharashtra, India

### ARTICLE INFO

#### Article history:

Received 15 May 2022

Received in revised form 7 June 2022

Accepted 8 June 2022

Available online 30 June 2022

#### Keywords:

CFD analysis; pulse tube cryocooler; viscous resistance; inertial resistance; oscillating flow; cryogenic temperature

### ABSTRACT

Pulse tube cryocoolers are extensively used for space application because of simplicity and reliability in operation. Many researchers have attempted the numerical analysis of the oscillatory flow inside the cryocooler, however, the precise predictions of the exact behavior of the gas inside the cryocooler using CFD has not yet been reported. While performing the CFD analysis of cryocooler, the values of inertial and viscous resistance coefficients play vital role and highly contributes to the pressure drop taking place in porous media. The prime objective of present work is to analyze the effect of these resistance values on performance of cryocooler. A single stage Stirling type pulse tube cryocooler model from literature is employed to perform the CFD analysis and the results obtained from the analysis are validated to ensure that methodology used for analysis is correct. The resistance values mentioned in the literature are applicable for steady and unidirectional flows. The model is further modified for the values of resistances for oscillating flow at room temperature and oscillating flow at cryogenic temperature. It is observed that performance predictions for oscillating flow at cryogenic temperature resistance values yields substantially lower temperature than all other cases. As experimental validation of this model is still not reported in literature, the reliability of accurate resistance values is not confirmed. Hence, another model of single stage Stirling type pulse tube cryocooler from literature is numerically analyzed for various operating conditions and is compared with its experimental performance, and found to be in fair agreement.

## 1. Introduction

Pulse tube cryocoolers are quite popular due to their simplicity in design and compact size. They are extremely reliable due to absence of moving parts at the cold end. Pulse tube cryocoolers are particularly suitable for applications in space, missile guiding systems in defence, medical application like cryosurgery and magnetic resonance imaging (MRI), superconducting electronics, liquefaction of nitrogen, and liquid nitrogen transportation. It uses the principle of pressurization and depressurization of gas to achieve the refrigeration effect at cold end of pulse tube [1-3].

\* Corresponding author.

E-mail address: [opjoshi\\_p19@me.vjti.ac.in](mailto:opjoshi_p19@me.vjti.ac.in) (Onkar Joshi)

<https://doi.org/10.37934/cfdl.14.6.7989>

Significant literature is available dealing with flow analysis inside the regenerator. However, very few researchers have performed the CFD analysis of complete pulse tube cryocooler. It is observed that the resistance values in the CFD analysis are oversimplified using unidirectional flow and room temperature conditions [4, 6-8]. The practical condition inside pulse tube cryocooler is oscillating flow at cryogenic temperature range. It is further observed that experimental validation of the results obtained from such CFD analysis are either pending [4] or not matching with experimental data [7-8] which made authors unable to draw any firm conclusions. To overcome these limitations, experimental and numerical analysis of the regenerator are performed and resistance values for oscillating flow at room temperature for various regenerator filler material are calculated [9-11]. The further investigations report about these resistance values for oscillating flow at cryogenic temperatures [12]. While performing CFD analysis, considering the local thermal equilibrium against non-equilibrium between the wire mesh material of porous media and working fluid yields the lower cycle average temperature of cold end, which is having negligible temperature difference with non-equilibrium condition at the cost of huge amount of time and computational facility [13]. In addition to that, performing the 3-D analysis of complete cryocooler takes too much computational time and highly sophisticated computational facilities. It is reported that the results obtained from such analysis have no significant difference than those obtained using axisymmetric model [14].

From the above literature review, it can be concluded that most of the investigations performed are of numerical type only, without any validation with experimental results. The results reported using CFD analysis of complete cryocooler with inertial and viscous resistance values do not reflect the actual working conditions of cryocooler considering oscillating flow at cryogenic temperatures. In view of this, the objective of present work is to develop a numerical analysis on complete single stage Stirling type pulse tube cryocooler model which uses the resistance values of oscillating flow at cryogenic temperatures under various working condition, including effect of cold end orientation.

## 2. Model Development

Cha *et al.*, [4] have performed CFD analysis of complete single stage Stirling type pulse tube cryocooler, which deals with viscous and inertial resistance values for unidirectional flow at room temperature. The present model is initially developed to validate the results by considering the boundary conditions and resistance values as same as those reported in [4]. ANSYS Fluent is employed to design the model and meshing. Axi-symmetric condition is used for analysis. Quadrilateral type of elements is used to reduce the complexity of analysis. Total number of nodes included is 4319. A User Defined Function is used to give sinusoidal pressure as input to the regenerator. This base model uses stainless steel mesh #325 as regenerator wire mesh material.

The regenerator, which is a porous medium, plays an important role in any cryocooler. To predict the realistic performance, it is vital to apply proper boundary conditions in the CFD model. The modelling of regenerator requires appropriate definition and knowledge about hydrodynamic parameters viz. viscous resistance, inertial resistance and porosity. In Stirling cryocoolers, both clear fluid region and porous region are present. The regenerator with wire mesh is modeled as a porous region. In the clear fluid region, the momentum equations and energy equations are directly solved. For the porous region, the volume averaging method is used to derive the macroscopic momentum and energy equations. The mass and momentum conservation equations for fluid flow in porous region can be written as [16]:

$$\epsilon \times \frac{\partial \rho}{\partial t} + \nabla \cdot (\rho \langle u \rangle) = 0 \quad (1)$$

$$\frac{\rho}{\varepsilon} \times \left\{ \frac{\partial u}{\partial t} + \frac{1}{\varepsilon} \langle u \rangle \cdot \nabla \langle u \rangle \right\} = -\nabla P + \mu \cdot \nabla^2 u - \nabla \cdot \rho \cdot \bar{u}' \cdot u' + S \quad (2)$$

The momentum source  $S$  is non-zero in the porous region and is given by:

$$S = -\left( \frac{\mu}{K} \langle u \rangle + \frac{C}{2} \cdot g |\langle u \rangle| \langle u \rangle \right) \quad (3)$$

where,  $\langle u \rangle$  is the volume averaged velocity;  $C$  and  $K$  are the inertial resistance and permeability of the porous media, respectively.

The energy equation for the porous medium can be written as:

$$(\rho \times Cp)_f \times \left\{ \frac{\partial(T)}{\partial t} + \langle u \rangle \cdot \nabla \langle Tf \rangle \right\} = \varepsilon \times \nabla \cdot (k_{eff} \times \nabla \langle Tf \rangle) \quad (4)$$

$$(\rho \times Cp)_f = \varepsilon \times (\rho \times Cp)_f + (1 - \varepsilon) \times (\rho \times Cp)_s \quad (5)$$

$$k_{eff} = \varepsilon \times k_f + (1 - \varepsilon) k_s \quad (6)$$

The preliminary model is validated by solving the above equation in CFD. Furthermore, the values of resistances for oscillating flow at room temperature as well as at cryogenic temperatures are also reported in literature [9,12]. Thus, two more cases are developed to analyze the effect of these resistance values on the performance of cryocooler. The resistances values used for analysis are listed in Table 1. While performing these analyses, every parameter was kept same except resistance value for ease of comparison between obtained results.

**Table 1**  
Cases for Different Resistance Values for Cha *et al.*, Model [4]

		Viscous resistance (m <sup>-2</sup> )	Inertial resistance (m <sup>-1</sup> )
Base case	Unidirectional flow at room temperature [4]	9.433×10 <sup>9</sup>	76090
Case 1	Oscillating Flow at room temperature [9]	1.56×10 <sup>10</sup>	67000
Case 2	Oscillating Flow at cryogenic temperature [12]	1.68×10 <sup>10</sup>	29700

Tendolkar *et al.*, [15] performed experimental analysis of single stage pulse tube cryocooler. Hence, the same model is used for CFD analysis. The dimensions and boundary conditions used for the analysis of model are listed in Table 2. The geometry and meshing are as shown in Figure 1 and 2. Taking from left to right, the components of cryocooler are Aftercooler (A), Regenerator (B), Cold End Heat Exchanger (C), Pulse Tube (D), Hot End Heat Exchanger (E), Inertance Tube (F) And Reservoir (G). A User Defined Function is developed to give sinusoidal pressure wave as input to the cryocooler at compressor exit. The working pressure is 16 bar and operating frequency is 54 Hz with pressure ratio of 1.5. Quadrilateral type of elements is adopted in the revised model as well. Total number of nodes after meshing is 8533.

**Table 2**  
Geometrical Details and Boundary Conditions

Component	Diameter (mm)	Length (mm)	Boundary conditions
Aftercooler	28	18	Isothermal wall at T=300K
Regenerator	28	54	Adiabatic wall
Cold end heat exchanger	12.2	18	Adiabatic wall
Pulse tube	12.2	80	Adiabatic wall
Hot heat exchanger	12.2	18	Isothermal wall at T=300K
Inertance tube	2.3	2200	Isothermal wall at T=300K
Reservoir	76	176	Convective wall with $h = 15 \text{ W/m}^2.\text{K}$

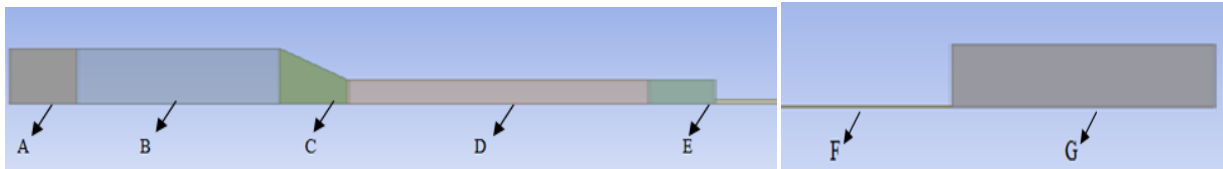


**Fig. 1.** Geometry of Tendolkar *et al.*, [15] model

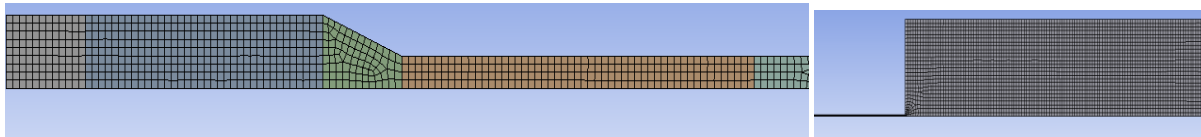


**Fig. 2.** Meshing of Tendolkar *et al.*, [15] model

During all the simulations, stainless steel #400 is considered as wire mesh material and helium gas is considered as working substance. It is necessary to consider the variation of properties of helium and stainless steel with respect to the temperature, especially for cryogenic range and higher operating pressures. Hence using the data from NIST WebBook [17], a higher order polynomial is fitted for dynamic viscosity and thermal conductivity of helium and stainless steel. The polynomial is valid for the temperature range of 20-350 K. The expressions obtained for helium gas are as follows:

$$\text{Dynamic Viscosity, } \mu = (1.195 \times 10^{-17}) T^5 - (1.133 \times 10^{-14}) T^4 + (4.1544 \times 10^{-12}) T^3 - (7.606 \times 10^{-10}) T^2 + (1.243 \times 10^{-7}) T + 1.991 \times 10^{-6} \quad (7)$$

$$\text{Thermal Conductivity, } k = -(1.051 \times 10^{-12}) T^4 + (1.376 \times 10^{-9}) T^3 - (8.43 \times 10^{-7}) T^2 + 0.0006 T + 0.0235 \quad (8)$$

Using the same analogy, the expressions for stainless steel are as follows:

$$\text{Specific Heat, } C_p = (3 \times 10^{-5}) T^3 - 0.0218 \times T^2 + 6.0689 \times T - 149.96 \quad (9)$$

$$\text{Thermal Conductivity, } k = (6 \times 10^{-7}) T^3 - 0.0004 \times T^2 + 0.1158 \times T + 1.0777 \quad (10)$$

Standard k-ε turbulence model with standard wall temperature is used. Aftercooler, cold and hot end heat exchangers and regenerator are modeled as porous media. Second order solution methods are adopted to have better accuracy. For this revised model, the results with unidirectional flow at room temperature are readily available [6]. Similar to the analysis performed for base case of Cha *et al.*, [4], different cases are developed in terms of the resistance values used for the simulations, as listed in Table 3.

**Table 3**

Cases for Different Resistance Values for Tendolkar *et al.*, [15] Model

	Viscous resistance (m <sup>2</sup> )	Inertial resistance (m <sup>-1</sup> )
Bhavin <i>et al.</i> , [6]	9.433×10 <sup>9</sup>	76090
Case A (Oscillating Flow at Room Temperature) [9]	3.95×10 <sup>10</sup>	120000
Case B (Oscillating Flow at Cryogenic Temperature) [12]	2.7×10 <sup>10</sup>	38600

The variations in charge pressure and cold end heat exchanger temperature are analyzed and reported by Perrella *et al.*, [12]. The values of operating pressure and minimum temperature for the revised model fall within the specified range, and hence acceptable to be directly employed. Further, to analyze the effect of gravity on the performance of cycle average temperature of cold end heat exchanger, three cases are made as listed in Table 4.

**Table 4**

Cases for Effect of Gravity on Tendolkar *et al.*, model [15]

Case details	
Case C	Resistance values for unidirectional flow at room temperature by Bhavin <i>et al.</i> , [6] model with cold end heat exchanger below hot end heat exchanger Temperature
Case D	Resistance values for Oscillating Flow at Cryogenic Temperature with cold end heat exchanger below hot end heat exchanger Temperature
Case E	Resistance values for Oscillating Flow at Cryogenic temperature with cold end heat exchanger above hot end heat exchanger Temperature

Numerical simulations are performed to ensure that the results obtained are independent of grids used for analysis. Another two models of using 12447 and 16655 number of nodes are created and simulations are performed. These models use the same working and boundary conditions as that of case B (See table 3) to ensure that results obtained are within acceptable limits.

### 3. Results and Discussion

Figure 3 shows the comparative cooldown curve for Cha *et al.*, [4] and present simulation results. It can be seen that simulation results of cycle average temperature at cold end heat exchanger to be 87.1 K against 86.9 K from Cha *et al.*, [4]. The variation in the initial slope of cooldown curve is attributed to the difference in the type of mesh. Cha *et al.*, [4] has reported to use dynamic mesh, whereas the base model developed employs UDF. It can be concluded that results obtained by simulations are in very nice agreement with actual results. Figure 4 shows the comparison of axial temperature distribution between Cha *et al.*, [4] and present analysis. Here as well, it seems the axial temperature distribution is in fine resemblance with Cha *et al.*, [4].

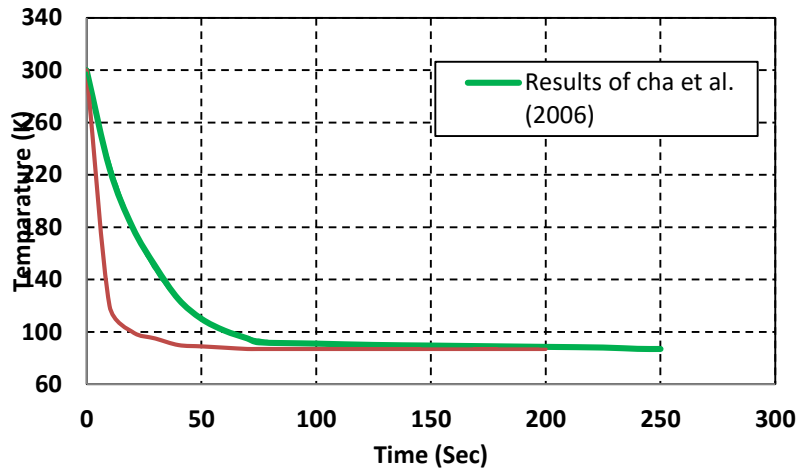


Fig. 3. Cooldown Curve

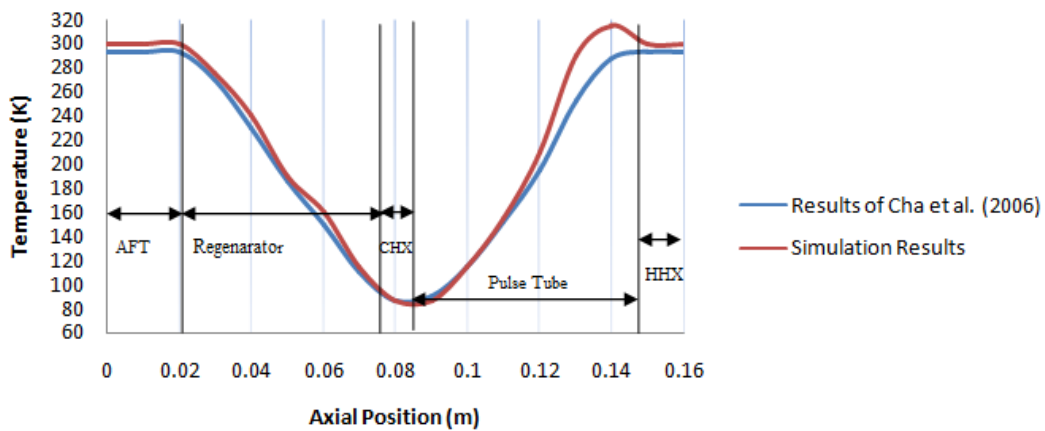


Fig. 4. Axial Temperature Distribution along Length of PTC

From figure 5, it can be seen that the cycle average temperature at cold end heat exchanger reaches 80 K for resistance value of oscillating flow at room temperature (case 1) while that for oscillating flow at cryogenic temperature (case 2) reaches 75 K. This clearly shows that the resistance values resembling to the experimental conditions yield significant difference from the steady flow resistance value at room temperature.

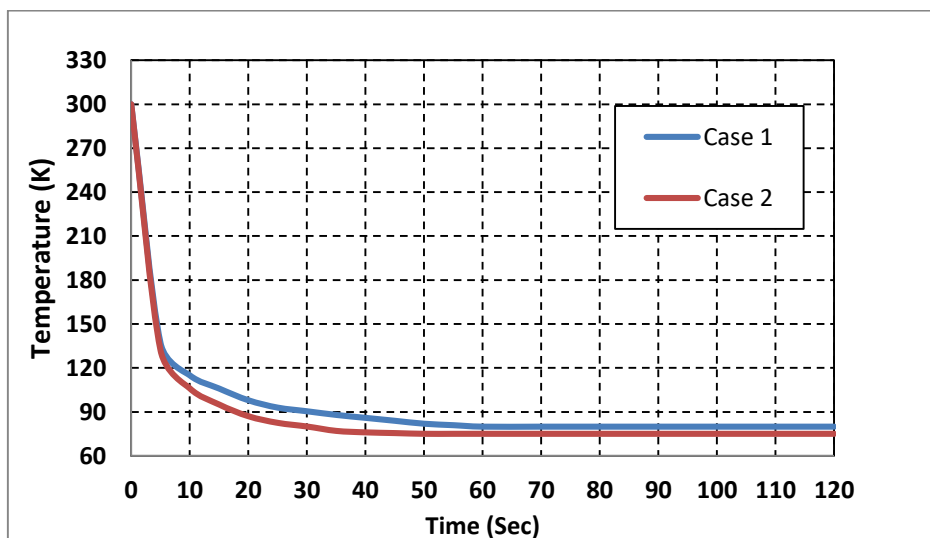


Fig. 5. Cooldown Curves at Different Resistance Values for Cha *et al.*, [4] model

Figure 6 shows the cooldown curve for cases listed in Table 3, i.e., towards investigations of resistance values for oscillatory flow and cryogenic temperature. Bhavin *et al.*, [6] has reported the steady state cycle average temperature of 46.4 K for same model. Case A reaches the steady state cycle average temperature of 40.4 K while case B reaches to 30.6 K. The experimental value [15] for the temperature of cold end heat exchanger is 54 K.

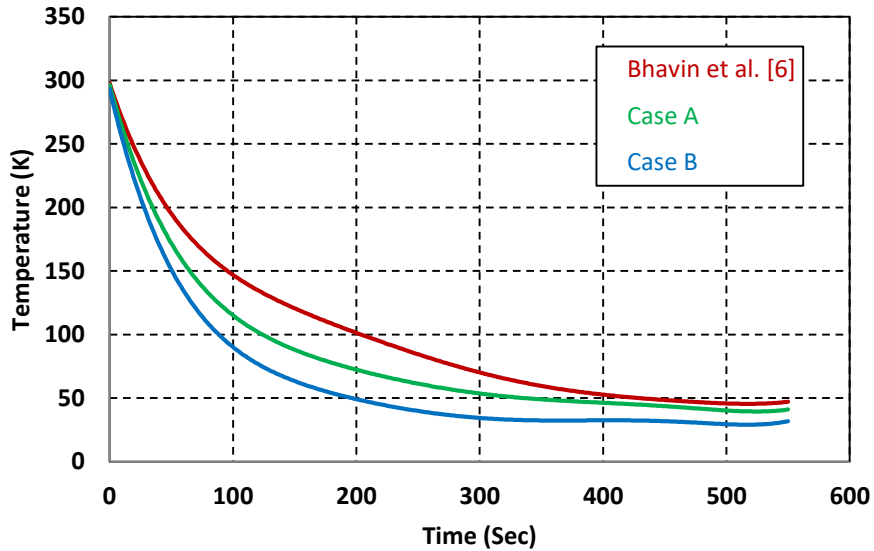


Fig. 6. Cooldown Curve for Tendolkar *et al.*, [15] Model for Different Resistance Values

For the cases listed in Table 4, i.e., towards investigations about effect of cold end orientation, analysis is executed and is shown in Figure 7. It can be seen that case C, i.e., cold end is below hot end and unidirectional flow at room temperature, yields steady state cycle average temperature of 48.2 K, while case D, i.e., cold end is below hot end and oscillatory flow at cryogenic temperature, results in steady state cycle average temperature of 32.2 K. It is interesting to note that Case E, i.e., cold end is above hot end and oscillatory flow at cryogenic temperature, reaches steady state cycle average temperature of 34.8 K.

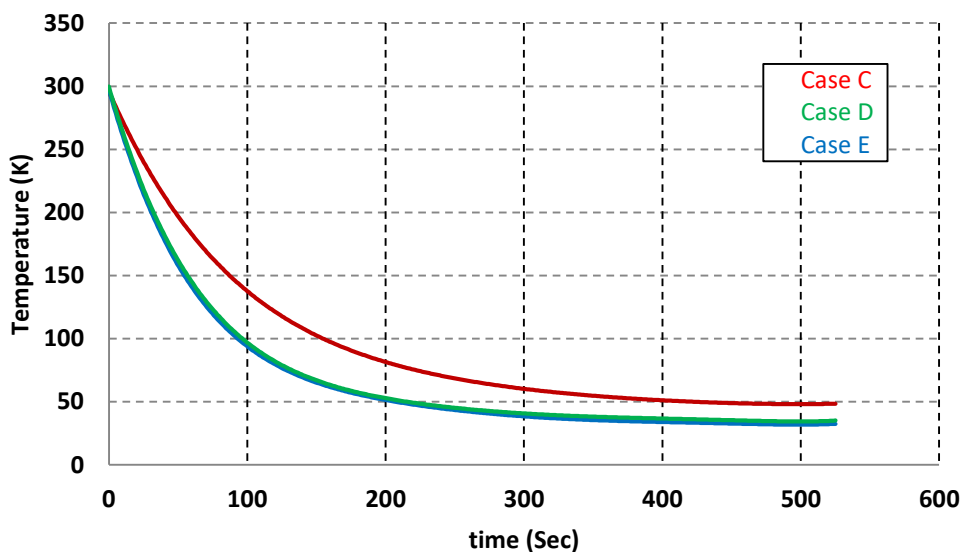
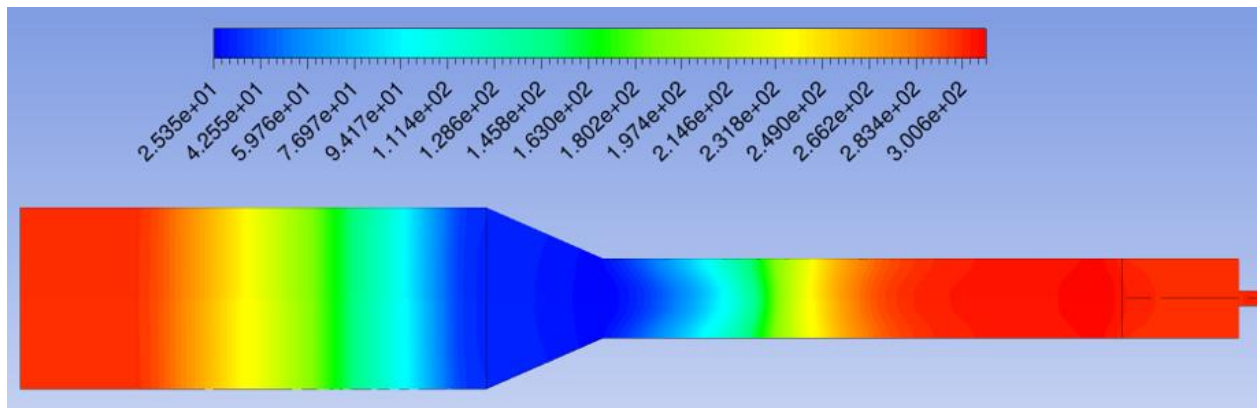


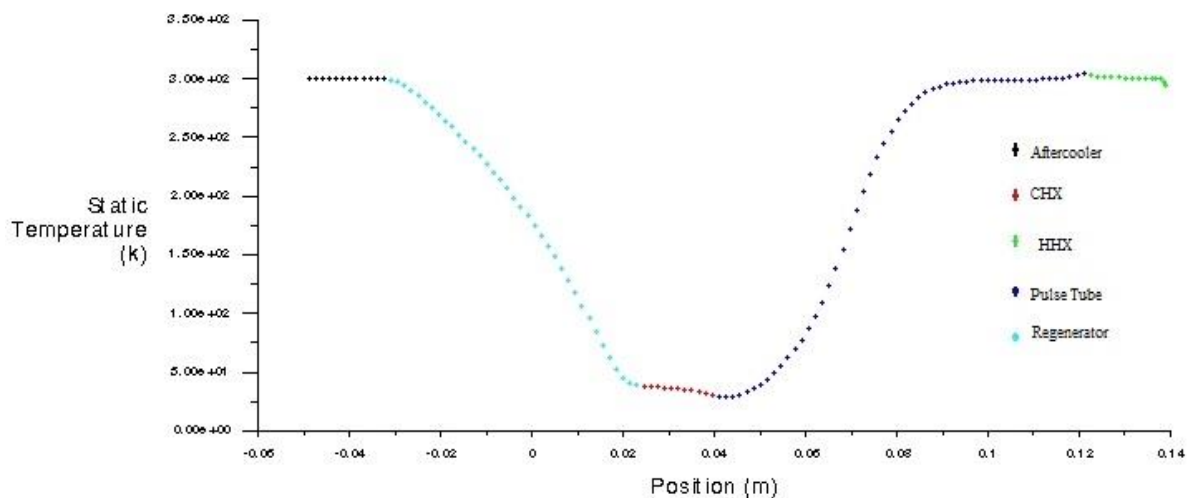
Fig.7. Cooldown Curve for Gravity Effect on Tendolkar *et al.*, [15] Model

Figure 8 shows the temperature contour plots for the simulation results of case B. For better understanding of temperature distribution, the part of inertance tube and reservoir are omitted. It can be clearly seen that the generation of lowest temperature at cold end of pulse tube and the temperature distribution along the length of regenerator, both as a validation of working principles of pulse tube cryocooler.



**Fig. 8.** Temperature Contour Plot for PTC

Axial temperature distribution along the entire length of pulse tube cryocooler (excluding inertance tube and reservoir) is shown in Figure 9. It can be also accepted as another form of validation of the dynamics of fluid flow inside the pulse tube cryocooler.



**Fig. 9.** Axial Temperature Distribution along Length of Cryocooler

The results obtained for grid independency test are shown in Figure 10. It can be observed that there is little difference between the steady state cycle average temperature obtained for all the three models using the different number of nodes. This confirms that the results obtained are reasonably grid independent. Thus, model using 8533 number of nodes is used for further analysis.

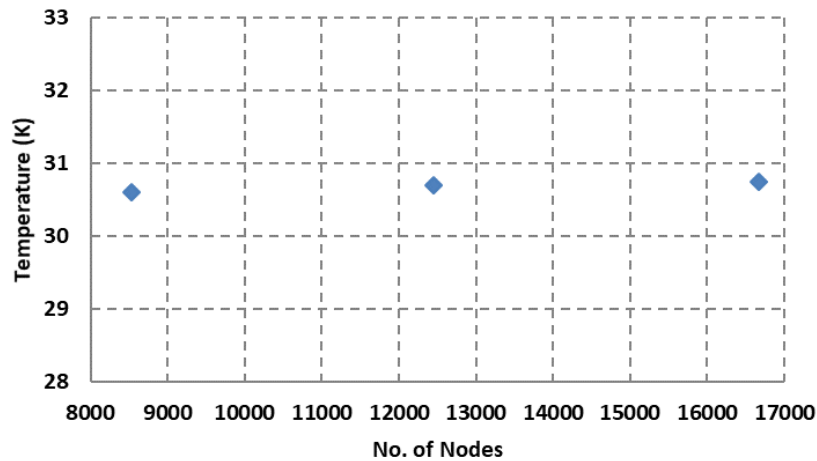


Fig. 10. Grid Independency Test

#### 4. Conclusions

The prime objective of present work is to investigate the effect of values of viscous and inertial resistances on the theoretical predictions about the performance of single stage Stirling type pulse tube cryocooler. Accordingly, a base model is created and successfully validated to set the methodology of numerical analysis. To overcome the lacuna of absence of experimental results against employment of the predicted resistance values, number of cases is developed to analyze the effect of change in resistance values at different working conditions. As expected, the resistance values for oscillating flow at cryogenic temperature yield lowest temperature of 75 K against the temperature of 86.9 K for the base case [4]. This emphasizes on the criticality of the accurate resistance values to be incorporated in the CFD simulations. As this model is having limitation of the experimental validation, another model from literature [15] is simulated by integrating appropriate resistance values for oscillating flow at cryogenic temperature. The selected are valid over the specified range of operating pressure and cold end heat exchanger temperature [12]. This simulation of complete cryocooler reports steady state cycle average temperature of 32.2 K at the cold end heat exchanger with oscillatory flow at cryogenic temperatures. This difference in the temperature obtained can be justified by following reasons:

- i. Slotted type of heat exchanger was used during the experimentation by Tendolkar *et al.*, [15] as the cold and hot end heat exchanger and aftercooler. In reality, modeling a 3-D slotted heat exchanger is quite cumbersome task so as to resemble the same geometrically in 2-D. Hence, in the actual simulations, this slotted type heat exchangers are made equivalent to a mesh matrix heat exchanger. However, the area available for heat exchange in case of mesh matrix is more which caused cold end heat exchanger to reach lower temperature than the experimental value.
- ii. In simulations, local thermal equilibrium is considered between matrix material and working fluid that is helium gas which assumed perfect heat transfer between matrix material and helium. In reality, there is always finite temperature difference between the matrix material and instantaneous gas temperature. This is attributed towards many aspects such as location of gas molecules at different time instances over the cycle, finite specific heat, finite thermal conductivity, etc. This yields further lower temperature at the cold end heat exchanger.

- iii. Helium is considered as ideal gas for its density model in CFD setup. Hence, real gas effects are suppressed which further affects cold end temperature value.
- iv. Wall thickness of all components is neglected which eliminates the loss due to axial heat conduction along the length of each component.

Considering the factors mentioned above, it ensures that the theoretical predictions and experimental results are within acceptable range. Finally, it can be concluded that, the simulation results obtained using resistance values for appropriate conditions validates their resemblance with the experimental results. This assists towards accurate temperature predictions while performing the simulations of a newly designed cryocooler. This, ultimately, helps in finalization of dimensions of various components of any pulse tube cryocooler with minimum iterations.

### Declaration of competing interest

Author declares that this article is not published any other journal or conference. Also, this research did not receive any specific grant from funding agencies in the public, commercial, or not-for-profit sectors.

### References

- [1] Milind\_D.\_Atrey (2020) , International Cryogenics Monograph Series , "Cryocoolers Theory and Applications", Springer Nature Switzerland AG . <https://doi.org/10.1007/978-3-030-11307-0>
- [2] Radebaugh, Ray. "A review of pulse tube refrigeration." *Advances in cryogenic engineering* (1990): 1191-1205.
- [3] Gifford, William E., and R. C. Longworth. "Pulse tube refrigeration progress." *Advances in cryogenic engineering* 10 (1965): 69-79.
- [4] Cha, J. S., S. M. Ghiaasiaan, P. V. Desai, J. P. Harvey, and C. S. Kirkconnell. "Multi-dimensional flow effects in pulse tube refrigerators." *Cryogenics* 46, no. 9 (2006): 658-665. <https://doi.org/10.1016/j.cryogenics.2006.03.001>
- [5] Harvey, Jeremy Paul. *Oscillatory compressible flow and heat transfer in porous media: application to cryocooler regenerators*. Georgia Institute of Technology, 2003.
- [6] Bhavin Shah, Deep Gudhka, Udeet Rangwala, Mandar Tendolkar and Arvind Deshpande, Vjti, Vjti Vjti. "Performance Investigations of Single Stage Stirling Type Pulse Tube Cryocooler with Inertance Tube Using Cfd Simulations." Proceedings of the Fortieth National Conference on Fluid Mechanics and Fluid Power December 12-14, NIT Hamirpur, Himachal Pradesh, India, 2013.
- [7] Choudhari, Mahmadrak S., B. S. Gawali, and Prateek Malwe. "Numerical Analysis of Inertance Pulse Tube Refrigerator." In *IOP Conference Series: Materials Science and Engineering*, vol. 1104, no. 1, p. 012008. IOP Publishing, 2021. <https://doi.org/10.1088/1757-899X/1104/1/012008>
- [8] Lokanath Mohanta, and M.D. Atrey, "Phasor Analysis of Pulse Tube Refrigerator Using CFD Analysis and Isothermal Model", Indian Journal of Cryogenics, Volume 35 A, Pages 356-361, (2010)
- [9] Cha, J. S., S. M. Ghiaasiaan, and C. S. Kirkconnell. "Oscillatory flow in microporous media applied in pulse-tube and Stirling-cycle cryocooler regenerators." *Experimental thermal and fluid science* 32, no. 6 (2008): 1264-1278. <https://doi.org/10.1016/j.expthermflusci.2008.02.008>
- [10] Landrum, E. C., T. J. Conrad, S. M. Ghiaasiaan, and Carl S. Kirkconnell. "Hydrodynamic parameters of mesh fillers relevant to miniature regenerative cryocoolers." *Cryogenics* 50, no. 6-7 (2010): 373-380. <https://doi.org/10.1016/j.cryogenics.2010.01.017>
- [11] Pathak, M. G., V. C. Patel, S. M. Ghiaasiaan, T. I. Mulcahey, B. P. Helvensteijn, A. Kashani, and J. R. Feller. "Hydrodynamic parameters for ErPr cryocooler regenerator fillers under steady and periodic flow conditions." *Cryogenics* 58 (2013): 68-77. <https://doi.org/10.1016/j.cryogenics.2013.10.002>
- [12] Perrella, Matthew, and S. Mostafa Ghiaasiaan. "Hydrodynamic resistance parameters of regenerator filler materials at cryogenic temperatures." *Cryogenics* 117 (2021): 103320. <https://doi.org/10.1016/j.cryogenics.2021.103320>
- [13] Shital Kumar Garg, B. Premachandran and Manmohan Singh, "Numerical Study of The Regenerator For a Miniature Stirling Cryocooler using The Local Thermal Equilibrium (LTE) and The Local Thermal Non-equilibrium (LTNE) Models", Thermal Science and Engineering Progress 11,150–161,2019. <https://doi.org/10.1016/j.tsep.2019.03.005>

- [14] Kumar, Pankaj, A. K. Gupta, R. K. Sahoo, and D. P. Jena. "Numerical investigation of a 3D inertance pulse tube refrigerator from design prospective." *Cryogenics* 98 (2019): 125-138.  
<https://doi.org/10.1016/j.cryogenics.2018.12.004>
- [15] Tendolkar, M. V., K. G. Narayankhedkar, and M. D. Atrey. "Performance Comparison of Stirling-Type Single-Stage Pulse Tube Refrigerators of Inline and 'U' Configurations." In *Proceedings of 15th International Cryocooler Conference*, pp. 209-215. 2008.
- [16] H K Versteeg and W Malalasekera, "An Introduction to Computational Fluid Dynamics", *Pearson Education Limited*, 2007.
- [17] NIST Chemistry WebBook, NIST Standard reference data
- [18] ANSYS Fluent User's guide, Release 12.0, 2009-01-29